UNRAVELING URBAN RAINFALL DYNAMICS: A 161-YEAR BAYESIAN DECOMPOSITION OF ABRUPT CHANGES, SEASONALITY, AND TRENDS IN JAKARTA, INDONESIA

***Fadilah Karamun Nisaa NADIYAH* [1], *Sri NURDIATI* [1*], *I Wayan MANGKU* [1], *Mohamad Khoirun NAJIB* [1] & *Syukri Arif RAFHIDA* [1]**

DOI: 10.21163/GT_2027.221.04

ABSTRACT

Rainfall variability in tropical urban regions remains challenging to characterize due to its strong spatiotemporal complexity and non-stationary behavior. This study investigates long-term rainfall dynamics in Jakarta, Indonesia, using the Bayesian Estimator of Abrupt Change, Seasonality, and Trend (BEAST) to analyze a 161-year monthly rainfall time series (1864–2024). The BEAST framework was used to decompose the rainfall series into trend, seasonal, and outlier components, allowing persistent structural changes to be distinguished from isolated extreme observations. The results indicate substantial temporal variability in Jakarta's rainfall regime. The most strongly supported candidate trend changepoint occurred around January 2020, with a posterior probability of 83.56% and an estimated abrupt change of 121.02 mm. The seasonal component exhibited its strongest candidate changepoints around January 2014 and January 2016, with posterior probabilities of 29.3% and 21.16%, respectively. The outlier component identified several isolated extreme observations, including January 1979, with an outlier changepoint probability of 92.49%, followed by January 1963 (82.72%), January 2002 (68.11%), January 1872 (67.92%), January 1965 (61.83%), and February 2020 (56.63%). Sensitivity analysis showed that explicitly accounting for isolated extreme observations increased the posterior support for the January 2020 trend changepoint from 71.04% to 83.56%, while its timing remained stable. These findings demonstrate that extreme observations can influence the strength of inferred structural changes and highlight the importance of probabilistic, non-stationary approaches for characterizing long-term rainfall dynamics in rapidly urbanizing tropical regions.

Keywords: *Bayesian Estimator of Abrupt Change, Seasonality, and Trend (BEAST); Changepoint detection; Rainfall variability; Outlier detection; Jakarta.*

1. INTRODUCTION

Climate change detection involves identifying systematic changes in observed climate variables while accounting for natural climate variability and external forcing. It also accounts for natural climate variability, such as the El Niño–Southern Oscillation, which occurs independently of external influences (Stott et al., 2021). Previous studies have investigated extreme events associated with climate change (Blain et al., 2011; Siliverstovs et al., 2010; van de Vyver, 2012; Gilleland et al., 2006). In recent decades, climate change has contributed to an increase in the frequency and intensity of extreme weather events. These include heatwaves, tropical storms, and extreme rainfall (WMO, 2021; Nurdiati et al., 2022; IPCC, 2023). Rainfall remains one of the most challenging climate variables to characterize because of its high spatial and temporal variability (Septiawan et al., 2017).

---

[1] *School of Data Science, Mathematics, and Informatics, IPB University, 16680 Bogor, Indonesia. fadilahkaramun.nisaa@apps.ipb.ac.id (FKNN), * Corresponding author nurdiati@apps.ipb.ac.id (SN); wayanma@apps.ipb.ac.id (IWM), mkhoirun@apps.ipb.ac.id (MKN), asrafhida@apps.ipb.ac.id (SAR).*

High-intensity rainfall events can lead to severe impacts (Zhou et al., 2023), including flooding, infrastructure damage, economic losses, and water contamination (Spekkers et al., 2017; Nguyen et al., 2021; Tu et al., 2023). Therefore, understanding rainfall variability is essential for developing effective mitigation and adaptation strategies (Koutsoyiannis and Baloutus, 2000).

Jakarta has experienced a significant increase in rainfall intensity over the past decades (Siswanto et al., 2016; Jannah et al., 2023; Maheng et al., 2024). For instance, extreme rainfall events that previously, under early 20th-century climate conditions, had a return period of 24.5 years, now occur much more frequently (Siswanto et al., 2017; Siswanto et al., 2015). Historical evidence indicates that extreme rainfall events have become more frequent, contributing to recurring flood disasters. The first major flood in Jakarta was recorded in 1918 (ANRI, 2003), followed by other major flood events in 1996, 2002, 2007, 2012, and 2014, most of which were driven by high rainfall intensity (Yunika et al., 2012; OCHA, 2013; Siswanto et al., 2015).

Jakarta is projected to experience a faster increase in extreme rainfall compared to other cities (Suroso et al., 2021; Siswanto et al., 2022). Historically, major floods were expected to occur once every five years, but recent evidence indicates that such events are becoming more frequent. This is reflected in a series of extreme rainfall events that triggered floods in 2015, 2018, and 2020 (Siswanto et al., 2017; Wicaksono and Herdiansyah, 2019; Patel, 2020). The trend appears to have continued in recent years, culminating in severe flooding and marked changes in rainfall patterns (Raidi, 2025; Anshory, 2025). Moreover, a shift in the timing of extreme rainfall events was observed, with major floods occurring in March and even extending into the dry season in July 2025 (Mardiana, 2025). These findings highlight significant changes in Jakarta's rainfall patterns in recent years, underscoring the urgency of conducting comprehensive analyses to detect rainfall pattern changes, particularly in Jakarta (Gure, 2021).

Various statistical approaches have been developed to detect changes in climate variables, including the Mann–Kendall test, Theil–Sen estimator, Pettitt test, regression-based approaches, and artificial intelligence methods (Knutson et al., 2017; Gocic and Trajkovic, 2013; Ribes et al., 2017; Maheng et al., 2024; Bône et al., 2022). However, conventional approaches may have limited ability to characterize nonlinear temporal dynamics and multiple structural changes in long-term climate records. More importantly, extreme observations may exert a strong influence on the identification and interpretation of structural changes when isolated events are not explicitly distinguished from persistent changes in the underlying signal. Consequently, an observed extreme event may either represent a short-lived anomaly or coincide with a broader shift in the rainfall regime, and distinguishing between these possibilities is important for interpreting long-term rainfall variability. These limitations make the interpretation of long-term rainfall dynamics sensitive to the treatment of nonlinear variation, structural changes, and extreme observations (Zhao et al., 2019).

To address these limitations, this study applies a Bayesian changepoint detection framework to one of the longest rainfall records in Southeast Asia. This framework offers probabilistic inference capable of capturing nonlinear patterns and detecting subtle changepoints. Bayesian inference treats parameters and model structures probabilistically, enabling more robust quantification of uncertainty (Dan'azumi et al., 2025). This study applies the Bayesian Estimator of Abrupt Change, Seasonality, and Trend (BEAST). This method enables probabilistic detection of changepoints and decomposition of time series into interpretable components, including trend and seasonality. In the present study, an outlier component is additionally incorporated to identify isolated observations that deviate substantially from the underlying trend-seasonal structure. This formulation provides a framework for examining whether extreme rainfall observations coincide with persistent structural changes or represent isolated departures from the underlying rainfall dynamics. Therefore, this study aims to characterize long-term rainfall variability in Jakarta over the 161-year period from 1864 to 2024 using the BEAST framework. Specifically, the study aims to (i) characterize the long-term trend and seasonal variability of monthly rainfall, (ii) identify probabilistic structural changepoints in the trend and seasonal components, and (iii) identify isolated extreme observations through the outlier component and examine their relationship with detected structural changes.

2. STUDY AREA AND DATA

The Jakarta metropolitan area is located on the northwestern coast of Java Island, at coordinates 6°12′ S–106°48′ E. As the capital of Indonesia, Jakarta plays a central role in the country's political and economic activities. Administratively, Jakarta is divided into five municipalities and one regency (**Fig. 1**). The region has experienced rapid population growth and urban expansion, with an annual growth rate of 0.94% (BPS, 2018). Accelerated urbanization has led to the emergence of informal settlements, increased transportation activity, and growing demand for residential and commercial space. These developments have significantly influenced local climate conditions (Januari et al., 2024).

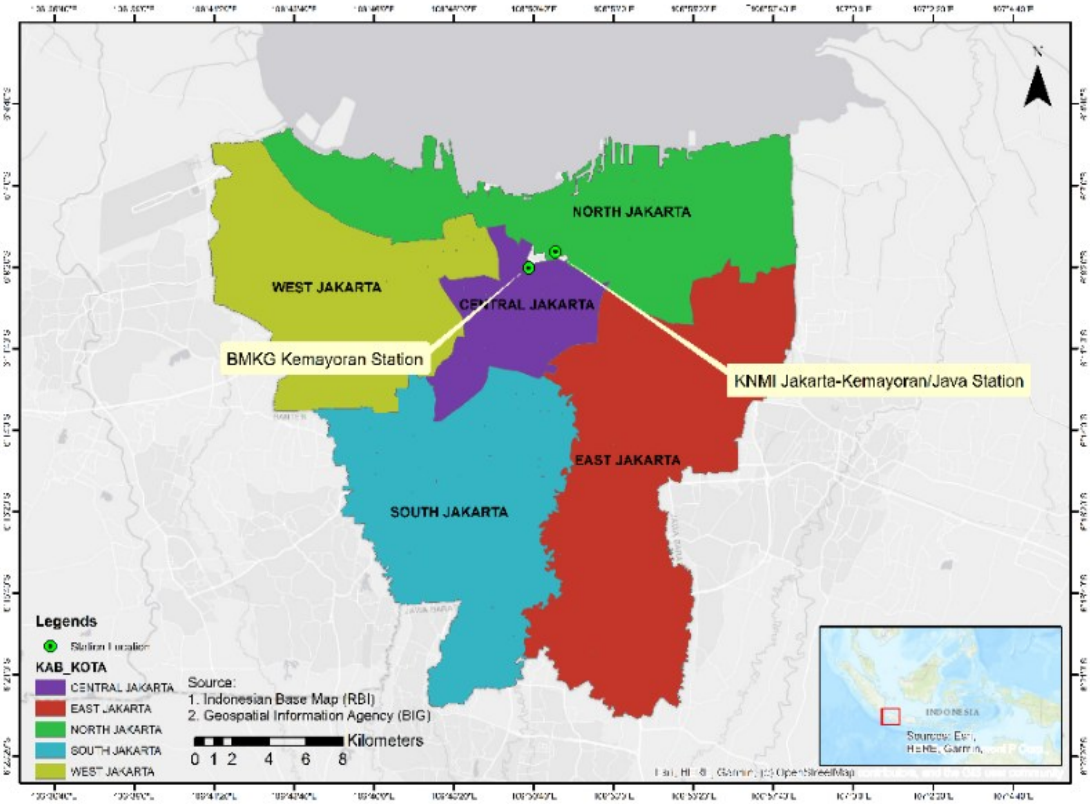

Fig. 1. Location of Jakarta, Indonesia, showing the administrative boundaries of five municipalities (Central, West, North, South, and East Jakarta) and the Thousand Islands Regency. Green dots indicate the observation stations: KNMI Jakarta–Kemayoran and BMKG Kemayoran.

Jakarta has a monsoonal rainfall regime, with relatively high rainfall during December–February and a pronounced dry period during June–August (Aldrian and Susanto, 2003). To investigate long-term rainfall variability, this study compiled monthly rainfall observations covering 161 years, from 1864 to 2024. The historical record consists of two observational sources. Rainfall observations from 1864–1990 were obtained from the archives of the Koninklijk Nederlands Meteorologisch Instituut (KNMI) at the Jakarta/Kemayoran station (−6.17°S, 106.82°E; elevation 7 m), whereas observations from 1991–2024 were obtained from the Meteorology, Climatology, and Geophysics Agency (BMKG) at the Kemayoran station (−6.16°S, 106.84°E; elevation 4 m). The two observation sites are geographically close, with an elevation difference of approximately 3 m (**Fig. 1**). The KNMI record was available as monthly accumulated rainfall, whereas the BMKG record consisted of daily rainfall observations.

Missing values in the BMKG daily rainfall records were reconstructed using an iterative multivariate linear regression imputation procedure. Missing observations were initially replaced with monthly mean values and subsequently updated through repeated ordinary least-squares regression until a complete dataset was obtained. The reconstructed daily BMKG rainfall data were then aggregated into monthly totals and merged with the monthly KNMI dataset to produce a continuous monthly rainfall record spanning 1864–2024. This procedure is conceptually related to iterative regression-based imputation methods (Templ et al., 2011).

Because the rainfall record was constructed from two observational sources, the consistency of the merged series was evaluated before subsequent time-series analysis. A Mann–Whitney test was first applied to compare rainfall distributions across the joining period between the KNMI and BMKG records. The test indicated a significant difference in median rainfall between the two periods ($p = 0.0008$). Such differences may reflect both climatic variability and potential non-climatic influences, including changes in station characteristics, instrumentation, observation procedures, or the surrounding environment (Aguilar et al., 2003). However, the two observation sites are located in close proximity and follow standardized rainfall measurement practices (BMKG, 2020; Setyawati et al., 2025), which reduces the likelihood that the observed difference can be attributed solely to the change in observational source.

To further assess whether the difference detected at the KNMI–BMKG transition represented a structural discontinuity caused by the data-source transition, a Pettitt test was subsequently applied to the complete merged rainfall series. Rather than detecting a changepoint at the 1990/1991 junction, the test identified a statistically significant changepoint around 1972 ($K = 80{,}263$; $p = 0.0094$). The detected changepoint therefore precedes the transition between the two observational sources by approximately two decades, suggesting that the principal structural change identified by the Pettitt test is unlikely to be explained solely by the merging of the KNMI and BMKG records. Instead, it may reflect longer-term hydroclimatic variability that occurred prior to the station transition.

The Mann–Kendall test further indicated a significant increasing trend in monthly rainfall over the full observation period ($S = 84{,}957$; $Z = 3.0001$; $p = 0.0027$). These preliminary assessments provide evidence that the 1864–2024 record contains both long-term trend and structural variability. Nevertheless, the conventional tests do not provide information on multiple changepoints, their posterior uncertainty, or the distinction between isolated extreme observations and persistent changes in the underlying rainfall signal. Therefore, the resulting continuous monthly series was subsequently analyzed using the BEAST framework described in Section 3.

This case study focuses on two main objectives. First, it applies an advanced methodological framework. Second, it establishes a foundation for identifying structural changes in rainfall. This framework can be extended in future studies to incorporate multiple drivers of climate variability. All analyses were conducted using MATLAB 2025a and RStudio, employing the Rbeast package for time series decomposition and changepoint detection.

3. METHODS

The methodological framework of this study examines Jakarta’s monthly rainfall over the period 1864–2024. To clarify the research workflow, the entire sequence of analytical steps is shown in **Fig. 2**, offering a visual overview of the process.

3.1. A Bayesian Estimator of Abrupt Change, Seasonal Change and Trend (BEAST)

The Bayesian Estimator of Abrupt Change, Seasonality, and Trend (BEAST) developed by Zhao et al. (2019). BEAST was selected due to its ability to simultaneously detect abrupt changes and model non-stationary climate dynamics, which are common in long-term rainfall records. This approach quantifies multiple sources of uncertainty. It also identifies abrupt changes across different temporal scales and captures complex nonlinear variations in time series data. Climate-related time series typically exhibit dynamics at three primary scales. These include (i) seasonal cycles, (ii) gradual long-term changes, and (iii) abrupt shifts caused by extreme events or climate regime transitions.

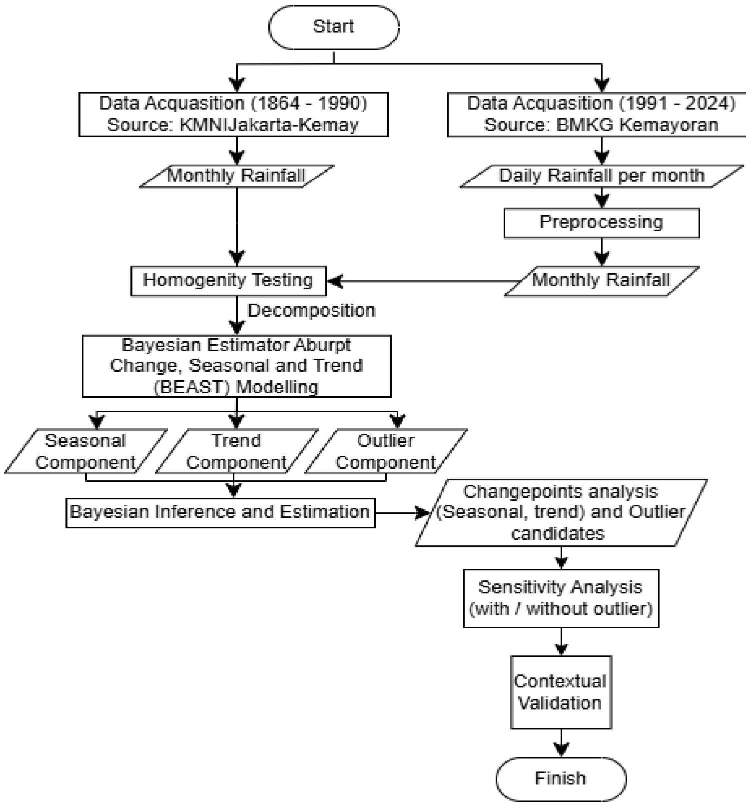

Fig. 2. Research workflow diagram.

In the decomposition framework, the observed time series is represented as the sum of a seasonal component, a trend component, an outlier component, and an error term. Abrupt structural changes are not represented as a separate additive component; instead, they are captured through changepoints within the seasonal and trend components. The outlier component is used to represent isolated observations that substantially deviate from the underlying trend-seasonal structure. The BEAST model applied in this study can therefore be expressed in Eq. (1).

$$\hat{y}(t_i) = f(t_i; \Theta) = S(t_i; \Theta_S) + T(t_i; \Theta_T) + O(t_i; \Theta_O) + \varepsilon_i, \qquad i = 1, \dots, n, \tag{1}$$

where,

$\hat{y}(t_i)$	-observed rainfall at time t_i;
$S(t_i; \Theta_S)$	-seasonal component;
$T(t_i; \Theta_T)$	-long-term trend component;
$O(t_i; \Theta_O)$	-outlier component representing isolated observations;
Θ_S and Θ_T	-parameters implicitly account for abrupt changes
$\varepsilon i \sim \mathcal{N}(0, \sigma^2)$	-error term with Gaussian noise.

The analysis employs the Rbeast package, which implements Bayesian estimation using the Markov Chain Monte Carlo (MCMC) algorithm (Zhao, 2025). The MCMC approach enables efficient exploration of a high-dimensional model space without incurring prohibitive computational costs. Consequently, it overcomes the limitations of analytical solutions and allows the Bayesian framework to address complexities that conventional methods may fail to capture. MCMC generates sample-based estimates that support statistical inference. In this study, it is used to evaluate the posterior distribution of the model parameters (Zhang et al., 2013).

3.2. MCMC Parameter Setup

During the simulation setup, several key parameters are specified, including the number of samples per chain, the number of chains, the burn-in period, and the thinning factor. Running multiple chains allows assessment of the convergence of the Markov Chain Monte Carlo (MCMC) algorithm toward the target posterior distribution. The burn-in period ensures that the chains reach a stable state before sampling begins, while the thinning factor is applied to reduce autocorrelation among successive samples.

These chains collectively capture essential information required to analyze rainfall patterns, including long-term trends, seasonal variations, and abrupt changes. Additional parameters include the maximum step size, resampling probabilities, and tolerance levels for credible intervals (CI).

3.2.1. Seasonal Component

The seasonal component $S(t)$ is approximated using a piecewise harmonic model defined over p changepoints ξ_k, where $k = 1, \dots, p$. These changepoints partition the time series into $(p+1)$ intervals $[\xi_k, \xi_{k+1}]$, with $\xi_0 = t_0$ and $\xi_{p+1} = t_n$ representing the temporal bounds of the dataset. The seasonal model is defined separately within each segment as follows in Eq. (2).

$$S(t) = \sum_{l=1}^{L_k} \left[a_{k,l} \cdot \sin\left(\frac{2\pi lt}{P}\right) + b_{k,l} \cdot \cos\left(\frac{2\pi lt}{P}\right) \right], \qquad \xi_k \le t \le \xi_{k+1};\; k = 0, 1, \dots, p, \tag{2}$$

where:

P	-seasonal period;
L_k	-the harmonic order in segment k;
$a_{(k,l)}$ and $b_{(k,l)}$	-coefficients of the harmonic basis functions;
p	-number of seasonal changepoints;
ξ_k	-temporal location of the k-th changepoint;

with,

$$\Theta_S = \{p\} \cup \{\xi_k\}_{k=1}^{p} \cup \{L_k\}_{k=0}^{p} \cup \{a_{k,l}, b_{k,l}\}_{k=0,\dots,p;;l=1,\dots,L_k}. \tag{3}$$

These parameters are estimated within the Bayesian framework, which allows probabilistic inference and robust uncertainty quantification. The seasonal harmonic order was allowed to vary between 1 and 5, while the number of seasonal changepoints was constrained to 0–10. A minimum separation of six monthly observations was imposed between adjacent seasonal changepoints. These settings allow changes in seasonal amplitude and structure to be identified while limiting unrealistically short seasonal segments.

3.2.2. Trend Component

The long-term trend component $T(t)$ is modeled as a piecewise linear function with m changepoints located at τ_j, where $j = 1, \dots, m$. These changepoints divide the time series into $(m+1)$ intervals $[\tau_j, \tau_{j+1}]$, with $\tau_0 = t_0$ and $\tau_{m+1} = t_n$. The trend model within each segment defined as in Eq. (4).

$$T(t) = a_j + b_j t, \qquad \tau_j \le t \le \tau_{j+1}, \qquad j = 0, 1, \dots, m. \tag{4}$$

where:

τ_j	-temporal location of the j-th changepoint;
a_j	-intercept of segment j;
b_j	-slope of segment j;
m	-number of trend changepoints,

with,

$$\Theta_T = \{m\} \cup \{\tau_j\}_{j=1,\dots,m} \cup \{a_j, b_j\}_{j=0,\dots,m}. \tag{5}$$

These parameters must be estimated to characterize the number and locations of structural changes, as well as the corresponding linear behavior within each segment. Estimating these parameters involves balancing model flexibility with interpretability. The polynomial order of the trend was restricted to 0–1, corresponding to constant or linear behavior within each segment. The number of trend changepoints was allowed to range from 0 to 50, with a minimum separation of six monthly observations between adjacent changepoints.

3.2.3 Outlier Component

An outlier component was incorporated to distinguish isolated extreme observations from persistent changes in the trend or seasonal components. In the BEAST framework, an observation may be represented by the outlier component when its deviation from the underlying trend-seasonal structure is sufficiently large relative to the estimated residual variation. The outlier component was enabled, with the number of potential outlier changepoints constrained to 0–10. The outlier detection threshold was controlled using an outlier significance factor of 2.5.

Outlier occurrence was evaluated probabilistically using the posterior outlier probability. Therefore, an observation identified by the outlier component is interpreted as an observation with posterior support for being an isolated departure from the underlying model, rather than automatically being treated as an erroneous measurement. This distinction is important for rainfall data because extreme precipitation may represent genuine meteorological events rather than measurement errors.

3.3. Parameter Strategies

In the BEAST framework, the full set of parameters $\{\Theta_S, \Theta_T, \Theta_O\}$ is partitioned into two categories for estimation, namely the model structure M and the parameter vector β_M, as shown in Eq. (6)**.** The model structure M defines the configuration of the time series decomposition including the number and temporal locations of trend and seasonal changepoints, the harmonic orders of the seasonal segments, and the configuration of the outlier component shown in Eq. (7). Conditional on a model structure, the parameter vector β_M contains the coefficients required to represent the corresponding trend and seasonal basis functions as defined in Eq. (8)**.**

$$\{\Theta_T, \Theta_S, \Theta_O\} = \{M, \beta_M\}. \tag{6}$$

$$M = \{m\} \cup \{\tau_j\}_{j=1,\dots,m} \cup \{p\} \cup \{\xi_k\}_{k=1,\dots,p} \cup \{L_k\}_{k=0,\dots,p} \cup M_O. \tag{7}$$

$$\beta_M = \{a_j, b_j\}_{j=0,\dots,m} \cup \{a_{k,l}, b_{k.l}\}_{k=0,\dots,p,l=1,\dots,L_k} \cup \beta_O. \tag{8}$$

After regrouping, the general linear BEAST model (Eq. (1)) defined in Eq. (9).

$$y(t_i) = x_M(t_i)\beta_M + \varepsilon_i. \tag{9}$$

where $x_M(t_i)$ represents the basis functions determined by the model structure M, including the trend and seasonal basis functions, while the outlier configuration is incorporated into the model structure, and ε_i denotes the residual error.

Model selection involves identifying the optimal model structure *M*. This includes determining the number and timing of changepoints as well as the appropriate level of harmonic complexity. This problem is analogous to variable selection in linear regression but is considerably more complex due to the combinatorial nature of possible model configurations. Therefore, this high-dimensional model selection problem is addressed within a Bayesian framework.

3.4. Bayesian Inference for Model Optimization

The Bayesian framework treats all unknown values as random variables, including the model structure M, the parameter vector β_M, and the residual variance σ^2. Given the observed data D, the objective is to estimate the posterior distribution of these quantities rather than relying on point estimates. According to Bayes' theorem, the posterior distribution is given by Eq. (10).

$$p(\beta_M, \sigma^2, M|D) \propto p(D|\beta_M, \sigma^2, M)\pi(\beta_M, \sigma^2, M), \tag{10}$$

with the likelihood function in Eq. (11) and prior distribution in Eq. (12):

$$p(D|\beta_M, \sigma^2, M) = \prod_{i=1}^{n} \mathcal{N}(y_i|x_M(t_i)\beta_M, \sigma^2). \tag{11}$$

$$\pi(\beta_M, \sigma^2, M) = \pi(\beta_M, \sigma^2|M)\pi(M), \tag{12}$$

where:

D	-the observed dataset;
M	-model structure;
β_M	-parameter vector under model M;
σ^2	-residual variance;
$p(D\|\cdot)$	-likelihood function;
$x_M(t_i)$	-basis functions defined by M;
$\pi(\beta_M, \sigma^2\|M)$	-conditional prior distribution;
$\pi(M)$	-prior distribution over model structures.

Due to limited prior information, a weakly informative prior is adopted. Specifically, a normal–inverse-gamma distribution is used for the conditional prior $\pi(\beta_M, \sigma^2 \mid M)$, allowing flexible modeling of parameter uncertainty. In addition, the prior $\pi(M)$ assumes that the number of changepoints follows a discrete distribution over non-negative integers with equal prior probability (Zhao et al., 2019).

The posterior distribution $p(\beta_M, \sigma^2, M \mid D)$is explored using a hybrid sampling approach. This approach combines Reverse-Jump MCMC for model selection with Gibbs sampling for parameter updates. This strategy enables efficient exploration of the posterior space while maintaining convergence and stability of the estimation process (Zhao et al., 2019).

4. RESULTS

4.1. Data Exploration

The monthly rainfall time series for Jakarta over the period 1864–2024 is presented in **Fig. 3**. The mean monthly rainfall is 157.66 mm, with a standard deviation of 137.07 mm, indicating substantial variability. Rainfall values range from 0 mm to 1,066.11 mm, reflecting the presence of both dry conditions and extreme precipitation events.

An increasing tendency in average monthly rainfall is observed toward the 2020s (**Fig. 3**). This trend provides a basis for further analysis of seasonal and long-term variations. Throughout the observation period, several extreme rainfall events exceeding 600 mm per month were identified. The most extreme event occurred in February 2020, when monthly rainfall reached 1,066.11 mm.

These results confirm that Jakarta's rainfall regime is strongly influenced by the monsoonal climate, consistent with Aldrian and Susanto (2003). Peak rainfall occurs during January and February, as shown in **Fig. 4**. Variability during these months is higher, as indicated by the wider interquartile range and longer whiskers in the boxplot.

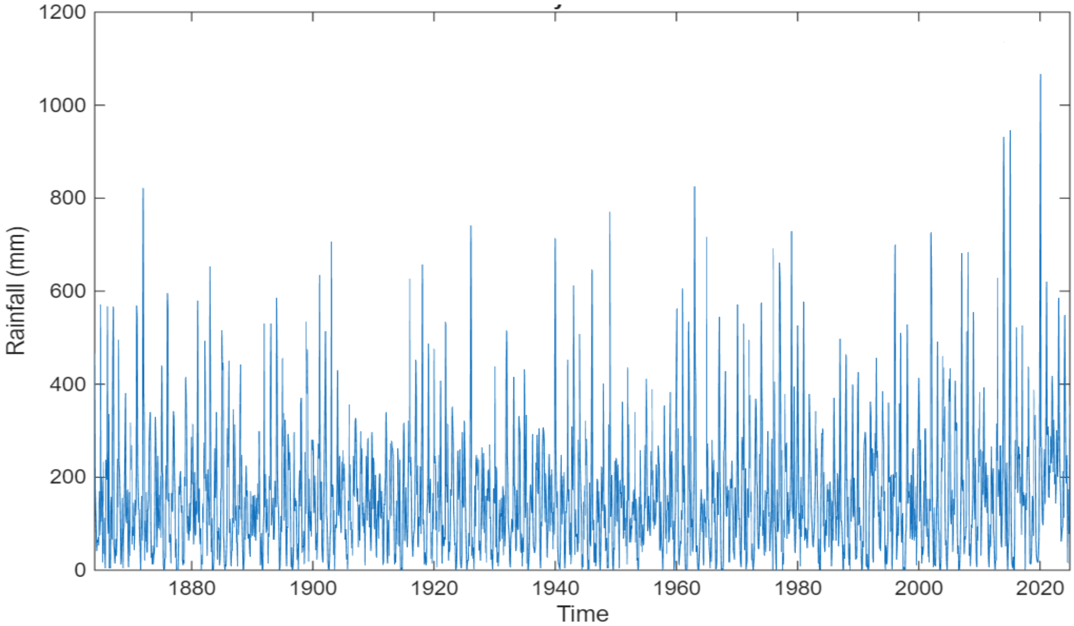

Fig. 3. Monthly rainfall time series (mm) in Jakarta for the period 1864–2024, illustrating long-term variability, seasonal fluctuations, and extreme events.

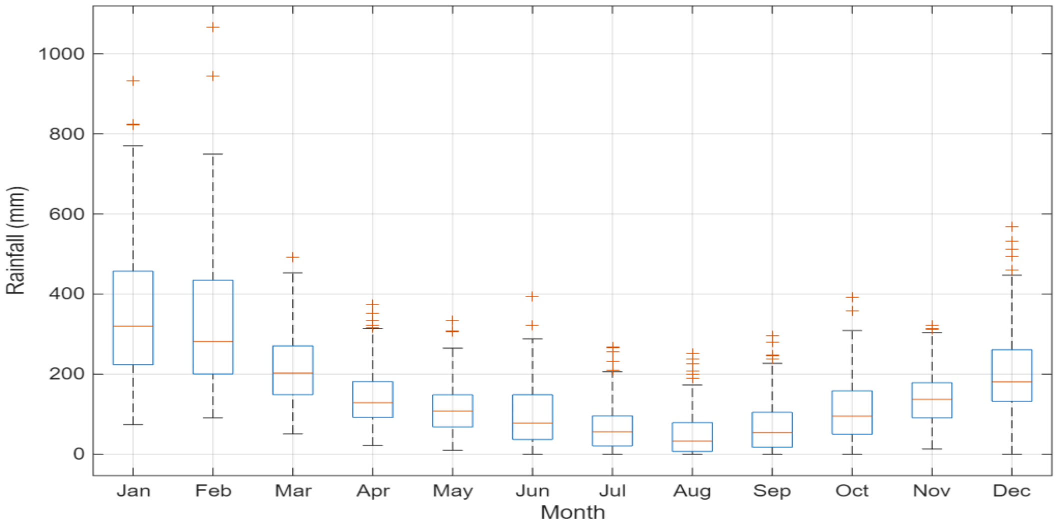

Fig. 4. Boxplot distribution of monthly rainfall (mm) in Jakarta for 1864–2024, showing the median, interquartile range (IQR), and outliers, highlighting strong seasonality with peak rainfall in January–February and minimum rainfall in August.

In contrast, the driest conditions occur in August and September, during which zero rainfall is occasionally observed. However, outliers are also present in these months, suggesting the occurrence of anomalous rainfall events during the dry season. These anomalies suggest increasing variability and potential shifts in seasonal rainfall behavior.

4.2. BEAST Results

The BEAST model was applied to Jakarta's monthly rainfall data to detect changepoints and estimate their associated probabilities, enabling the characterization of long-term rainfall dynamics. The dataset consists of 1,932 observations with a regular monthly temporal resolution. The time series was decomposed into seasonal, trend, and outlier components, as expressed in Eq. (13):

$$y(t) = S(t) + T(t) + +O_t + \varepsilon(t). \tag{13}$$

Three independent chains were run, with 3,000 retained samples per chain, a burn-in period of 150 iterations, and a thinning factor of 1. The random-number seed was fixed at 123 to ensure reproducibility. Based on this configuration, the total number of explored candidate structures is given in Eq. (14).

$$N = (\text{burnin} + \text{samples} \times \text{thinning factor}) \times \text{number of chains}. \tag{14}$$

With these settings, the total number of MCMC iterations across the three chains was 9,450, including the burn-in iterations. The maximum changepoint movement step was set to 12 observations. The resampling probabilities for the trend and seasonal polynomial/harmonic orders were set to 0.10 and 0.17, respectively. Posterior credible intervals were calculated at the 95% level. The seasonal and trend components were constrained to have a minimum segment length of six monthly observations, while the first and last six observations were excluded from consideration as changepoint locations.

The final BEAST model achieved an R^2 of 0.5814 and RMSE of 88.86 mm. These values indicate a reasonable in-sample representation of the observed rainfall series. The fitted model explicitly include an outlier component, allowing isolated extreme observations to be distinguished from persistent structural changes in the trend and seasonal components.

Fig. 5 presents the BEAST decomposition results provide a comprehensive representation of Jakarta's rainfall dynamics. The top panel shows the original time series (black), while the second panel (red) illustrates the seasonal component with the probability of changepoints (third panel). Seasonal component characterized by sinusoidal fluctuations that reflect recurring annual patterns in rainfall intensity. The fourth panel (green) shows the trend component with the probability of changepoints (fifth panel), whereas describes longer-term temporal variation. The sixth panel illustrates the direction (slope) of change in the trend component, where red indicates an increasing trend, green denotes stability, and blue represents a decreasing trend. The inclusion of the outlier component (last panel) allows isolated departures from these underlying structures to be represented separately.

The decomposition indicates that rainfall dynamics were relatively stable over much of the early record, followed by increasingly dynamic behavior during the later decades. The posterior distribution of the model structure indicates that for the trend component. The posterior mean number of changepoints was 2.47, with a median and mode of 2, while the 90th percentile was four. These indicating uncertainty in the number of structural changes beyond the two most probable changes.

For the seasonal component, the posterior distribution provides weaker evidence for persistent seasonal structural changes than for trend changes. The posterior mean number of changepoints was 0.625, with a median and mode of 0, while the 90th percentile was 2. Nevertheless, individual candidate seasonal changepoints receive non-negligible posterior support. This indicates that the evidence for seasonal structural changes is concentrated around specific periods rather than supporting a uniformly changing seasonal regime throughout the 161-year record.

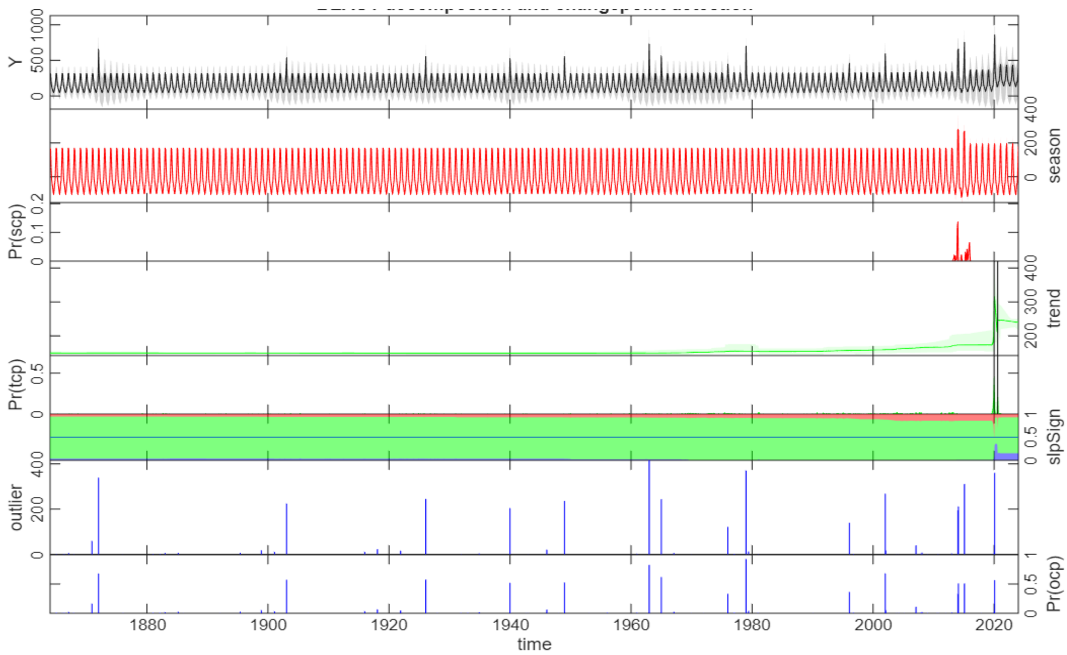

Fig. 5. Time series decomposition and changepoint detection using the BEAST model, showing the original data, seasonal component, trend component, structural changes, and outlier component.

4.2.1. Seasonal Component

The seasonal component exhibits a pronounced annual cycle throughout the observation period. The strongest positive seasonal contributions occur during January and February and the lowest contributions occurring during the dry-season months. The seasonal signal remained relatively stable until the early 2000s. The posterior changepoint probabilities were therefore used to rank candidate seasonal changepoints rather than treating all potential changepoints as equally supported.

As summarized in **Table 1**, the major scp were identified. The strongest posterior supported seasonal transition occurred in January 2014, with a posterior probability of 29.33% and an estimated abrupt change of 214.28 mm. The 95% credible interval for its timing extends from approximately July 2013 to January 2014. A second seasonal changepoint was identified in December 2015, with a posterior probability of 21.16% and an estimated abrupt change of 79.20 mm. Its 95% credible interval extends from approximately June 2015 to January 2016. A lower-probability candidate was detected around August 2014, with a posterior probability of 3.54% and an estimated negative change of 36.27 mm.

The magnitude of the estimated change in January 2014 is substantially larger than that associated with the December 2015 changepoint. This indicates that the 2014 transition represents the stronger modification of the seasonal structure, whereas the later 2015 transition is more appropriately interpreted as a subsequent adjustment of the seasonal regime. Importantly, these posterior probabilities represent uncertainty in the occurrence of individual changepoints, they should not be interpreted as conventional hypothesis-testing significance levels.

Table 1.

Seasonal changepoints detected by the BEAST model for Jakarta (1864–2024).

scp	Year	Month	Prop	Abrupt change (mm)	Credible Interval
1	2014	January	0.293	214.28	July 2013–January 2014
2	2015	November	0.212	79.20	June 2015–January 2016
3	2014	August	0.035	-36.27	May–October 2014

4.2.2. Trend Component

The reconstructed trend suggests relatively weak changes during the early portion of the record, followed by increasingly dynamic behavior during the latter part of the 20th century and especially after 2010. The sixth panel (**Fig. 5**) illustrates the direction of change in the trend component, whereas the trend remained relatively stable until the 1980s, as indicated by the predominance of green shading. After this period, an increasing trend becomes evident. Thereafter, the increasing extent of red shading reflects a gradual upward trend that persisted into the 2010s. A second upward phase is observed around 2020, following the seasonal changepoints identified earlier. However, this is followed by a transition toward a declining trend, as indicated by the emergence of blue shading.

The posterior distribution of the trend changepoint number indicates a median and modal value of two changepoints, with a 90th percentile is four changepoints. This demonstrates that the posterior distribution retains uncertainty regarding additional structural changes. Consequently, the candidate changepoints should be interpreted according to their posterior probabilities rather than as a fixed set of independent regime shifts.

Table 2 presents the highest-ranked candidates tcp with probabilities greater than 4%, representing the most strongly supported structural shifts identified by the BEAST model. The most strongly supported candidate changepoint in January 2020, with a posterior probability of 83.56% and a 95% credible interval spanning approximately July 2019 to January 2020. This changepoint was associated with an estimated upward shift in the trend component of 121.02 mm relative to the preceding period. Another notable changepoint was identified in August 2020, with a posterior probability of 25.46% and a credible interval extending from approximately July to October 2020, corresponding to an estimated positive shift of 36.06 mm. Earlier candidate changepoints were detected around February 2013 (7.12% probability), December 2003 (5.99%), and December 2007 (4.66%), although their abrupt changes were substantially smaller than those associated with the 2020 transition.

Table 2.

Trend changepoints detected by the BEAST model for Jakarta (1864–2024).

tcp	Year	Month	Prop	Abrupt change (mm)	Credible Interval
1	2020	January	0.8356	121.02	July 2019–January 2020
2	2020	August	0.2546	36.06	July–October 2020
3	2013	Feb	0.0712	0.56	August 2012–August 2013
4	2003	December	0.0599	0.68	February 2003–March 2004
5	2007	December	0.0466	0.35	June 2007–March 2008
6	1975	July	0.0436	0.34	May–October 1975

4.2.3. Outlier Component

The outlier component was included to distinguish isolated extreme observations from persistent changes in the underlying trend and seasonal structures. Unlike the trend and seasonal components, which represent persistent temporal structures and their associated changepoints, the outlier component is intended to capture localized departures at individual observations. Therefore, candidate outlier locations are not interpreted as changes between persistent rainfall regimes. Several individual observations received substantial posterior support for being isolated departures from the underlying trend-seasonal structure.

The posterior distribution of the outlier component identified several candidate outlier locations across the 161-year observation period. The highest posterior support was obtained for January 1979, with an outlier changepoint probability of 92.49%, followed by January 1963 with a probability of 82.72% (**Table 3**). Other candidate locations included January 2002 (68.11%), January 1872 (67.92%), and January 1965 (61.83%). The February 2020 observation also received substantial posterior support, with an outlier changepoint probability of 56.63%.

Table 3.

Highest-ranked candidate outlier locations identified by the BEAST model for Jakarta (1864–2024).

Rank	Year	Month	Outlier changepoint probability
1	1979	January	0.9249
2	1963	January	0.8272
3	2002	January	0.6811
4	1872	January	0.6792
5	1965	January	0.6183
6	1926	February	0.5751
7	1903	February	0.5721
8	2020	February	0.5663
9	1949	January	0.5269
10	1940	January	0.5206

The distribution of candidate outlier locations across different periods indicates that isolated departures from the underlying rainfall structure are not restricted to the most recent part of the record. In particular, the high posterior support for several observations before 2000 suggests that extreme deviations have occurred throughout the historical record rather than being a phenomenon exclusive to recent decades.

The February 2020 observation is of particular interest because it corresponds to the maximum monthly rainfall recorded in the dataset, at 1,066.11 mm. Its posterior outlier changepoint probability of 56.63% indicates that the observation received substantial support as a localized departure from the underlying trend-seasonal structure. However, this result should not be interpreted as evidence that the February 2020 event caused the January 2020 trend changepoint. Instead, the two results describe different aspects of the time series: the trend changepoint represents a potential change in the underlying long-term rainfall behavior, whereas the outlier component identifies an observation that is unusually large relative to that underlying structure.

4.3.4 Sensitivity of BEAST Results to the Outlier Component

To assess the robustness of the detected changepoints to the treatment of extreme observations, the BEAST model was fitted under two specifications: without an explicit outlier component and with an outlier component. The comparison presents in **Table 4**, focused on the posterior probabilities and magnitudes of the principal trend and seasonal changepoints.

The inclusion of the outlier component reduced the posterior support for the most strongly supported candidate trend changepoint around January 2020. Without the outlier component, the January 2020 changepoint had a posterior probability of 71.04% and an estimated abrupt change of 55.96 mm. After including the outlier component, the same changepoint remained identifiable around January 2020, but its posterior probability decreased to 83.56%, with an estimated abrupt change of 121.02 mm. This reduction indicates that the exceptionally large rainfall observations around the 2019–2020 period contribute to the statistical evidence for the detected trend transition. However, the persistence of the changepoint after explicitly accounting for outliers indicates that the transition is not entirely attributable to isolated extreme observations.

A similar pattern was observed for the seasonal component. The dominant seasonal changepoint remained around January 2014 under both model specifications, although its posterior probability decreased from 53.17% without the outlier component to 29.3% when the outlier component was included. The second seasonal transition also remained around 2015–2016, with its posterior probability decreasing from 25.06% to 21.16%. Thus, accounting for isolated extreme observations weakened the posterior evidence for the detected seasonal transitions but did not change their approximate timing.

The model including the outlier component also produced a lower RMSE (88.86 mm) than the model without the outlier component (95.08 mm), together with a higher R^2 (0.581 compared with 0.519). This indicates that explicitly accounting for isolated extreme observations improved the representation of the observed rainfall variability. Overall, the sensitivity analysis demonstrates that the principal changepoints identified by BEAST are partly influenced by extreme observations, particularly around 2020, but their temporal patterns remain broadly identifiable after the outlier component is incorporated.

Table 4.

Sensitivity of the principal changepoints to the outlier component

Component	Changepoint	Model	
		No outlier	With outlier
Model fit	RMSE (mm)	95.08	89.10
	R^2	0.519	0.581
Trend	January 2020	71.04% / 65.61	83.56% / 121.02
Seasonal	January 2014	53.17% / 251.17	29.3% / 214.28
	January 2016	25.06% / 160.07	21.16% / 79.20

Note: For changepoints, values are reported as posterior probability (%) / abrupt change (mm).

The model including the outlier component provided a better in-sample representation of the observed rainfall variability, as indicated by the lower RMSE and higher R^2. At the same time, the reduction in posterior probabilities and abrupt-change magnitudes demonstrates that the treatment of extreme observations affects the strength of evidence for the detected changepoints, particularly around 2020.

5. DISCUSSION

The BEAST analysis reveals that Jakarta's monthly rainfall exhibits pronounced non-stationary behavior characterized by both gradual trends and abrupt structural changes. The most strongly supported candidate trend transition was identified around January 2020, with a posterior probability of 83.56% in the final model that explicitly accounts for isolated outliers. The seasonal component exhibited two principal transitions around January 2014 and January 2016, with posterior probabilities of 29.3% and 21.16%, respectively. These probabilities should be interpreted as measures of posterior support for candidate changepoint locations rather than as deterministic evidence of a climate-regime transition. The results therefore indicate that rainfall dynamics in Jakarta have changed over time, while also demonstrating substantial uncertainty in the exact timing and strength of these structural changes.

The detected changepoints correspond closely with documented hydrometeorological events, providing empirical support for model results. In particular, the high-probability changepoints around 2012–2014 coincide with major flood events reported in Jakarta, while the 2019–2020 transition aligns with one of the most extreme rainfall episodes in recent decades. This temporal agreement highlights the ability of the BEAST framework to detect structurally meaningful changes that are not merely statistical artifacts but reflect real-world climate variability.

The temporal correspondence between the detected changepoints and documented hydrometeorological events provides useful contextual support for their interpretation. The seasonal transition around 2014 occurs close to a period characterized by major rainfall and flooding events in Jakarta, while the subsequent transition around 2016 follows the exceptional hydroclimatic conditions observed during 2015. The relatively large abrupt change associated with the 2014 seasonal transition (214.28 mm) compared with that of the 2016 transition (79.20 mm) suggests that the first transition represents the more substantial modification of the seasonal rainfall structure. The later transition may therefore represent an adjustment or stabilization of the seasonal regime rather than the emergence of an entirely independent seasonal pattern. This interpretation is consistent with the finding of An et al. (2023), who showed that seasonal rainfall variability over Indonesia is strongly modulated by ENSO, with changes in rainfall intensity and frequency occurring across different ENSO phases. The exceptional hydroclimatic conditions during 2015 were also associated with the concurrent influence of a strong El Niño, a positive Indian Ocean Dipole, and suppressed Madden–Julian Oscillation activity (Islam et al., 2018). Although these studies provide a plausible climatological context for the detected seasonal transitions, the present analysis does not directly test the relationship between the changepoints and ENSO or IOD indices. Therefore, the observed temporal correspondence should not be interpreted as evidence of direct causality.

The long-term trend provides additional evidence of substantial temporal variability in Jakarta rainfall. The reconstructed trend indicates relatively limited changes over much of the earlier record, followed by increasing variability and more pronounced trend changes from the latter part of the twentieth century onward. Notably, an early structural change identified by BEAST occurs around 1972–1973 (with probability 3.9%), closely corresponding to the significant changepoint detected independently by the Pettitt test around 1972. This temporal agreement is important because the Pettitt test identifies the same broad period without relying on the BEAST decomposition. The period also coincides with the strong 1972 El Niño, which was associated with substantial reductions in rainfall over Indonesia through changes in sea-surface temperature, Walker circulation, and atmospheric convection (Iskandar et al., 2019). Thus, the correspondence between the statistical changepoints and the documented 1972 hydroclimatic anomaly provides supporting evidence that the detected structural change is not necessarily an artifact of the statistical decomposition. Nevertheless, the present study does not establish that the 1972 El Niño caused the detected change. This pattern is consistent with regional observations across Mainland Southeast Asia, where increased atmospheric moisture and intensified monsoon dynamics have contributed to higher rainfall variability since the late 20th century (Skliris et al., 2022).

The most recent trend transition around January 2020 requires particular consideration because it coincides with an exceptionally wet period in Jakarta. The January–February 2020 period included extreme rainfall observations, with February 2020 recording the highest monthly rainfall in the observational series at 1,066.11 mm. The event therefore represents an important potential influence on the estimated structural change. The atmospheric conditions associated with the extreme rainfall in early 2020 have previously been linked to the interaction of a cross-equatorial northerly surge, equatorial waves, and an active Madden–Julian Oscillation (MJO), which enhanced moisture convergence over northwestern Java (Lubis et al. 2022). Muhammad et al. (2021) likewise demonstrated the important role of the Madden–Julian Oscillation in modulating extreme rainfall over Indonesia. These findings are particularly relevant to the present study because the strongest recent structural changes occur close to the period containing the exceptional rainfall observed in early 2020. Rather than treating the extreme event as synonymous with a structural changepoint, the results suggest that short-lived extreme rainfall and longer-term changes in the underlying rainfall structure may coexist.

This distinction is further supported by the sensitivity analysis. When the outlier component was incorporated into BEAST, the statistical support for the 2020 trend transition was reduced, indicating that the extreme observations around this period contribute to the strength of the detected structural signal. However, the transition was not completely removed. This suggests that the 2020 change cannot be interpreted simply as the consequence of a single record-breaking rainfall observation. Instead, the extreme event appears to be superimposed on a period in which the underlying rainfall behavior was also changing. This interpretation is consistent with the broader climatological literature showing that extreme precipitation events can arise from short-term atmospheric processes while occurring within longer-term changes in rainfall variability (Lubis et al., 2022; Muhammad et al., 2021).

In addition to large-scale climate influences, rapid urbanization in Jakarta may have contributed to localized modifications in rainfall patterns. On a global scale, sustained warming since the 1970s has increased atmospheric moisture and made extreme rainfall events more likely (IPCC, 2014). Similar patterns have been observed in the United States (Knutson et al., 2013a; Kunkel et al., 2013; Sillmann et al., 2013), Australia and the Western Pacific (Knutson et al., 2013b), Korea (Min et al., 2014), and across the broader tropical belt (Berg et al., 2009). Urban heat island effects, land-use changes, and increased surface roughness can alter atmospheric convection and precipitation processes. The interaction between global climate variability and local urban processes may therefore amplify the complexity of rainfall dynamics observed in the time series.

From a methodological perspective, the results demonstrate the importance of distinguishing structural changes from isolated extreme observations when analyzing long historical rainfall records. A conventional changepoint analysis may identify a strong transition around an extreme event without distinguishing whether the event represents a persistent change in the underlying process or an isolated departure. By incorporating an explicit outlier component, BEAST provides a means of evaluating this distinction probabilistically. The sensitivity analysis in the present study shows that the strength of the detected recent transition changes when extreme observations are treated separately, emphasizing the importance of accounting for exceptional events when interpreting long-term rainfall changes.

These findings highlight the importance of adopting flexible, non-stationary frameworks in flood risk assessment and infrastructure design to account for sudden shifts in rainfall patterns driven by climate change. In particular, reliance on conventional stationary assumptions may lead to systematic underestimation of flood risk in rapidly urbanizing regions such as Jakarta, underscoring the need to incorporate non-stationary modeling approaches into urban climate risk assessment frameworks.

Despite these contributions, several limitations should be acknowledged. This study relies on a single-station rainfall dataset, which may not fully capture spatial variability across the Jakarta metropolitan area. Additionally, the analysis focuses on statistical detection of changepoints without explicitly attributing them to specific physical drivers. Future research should integrate multi-station datasets, climate indices, and land-use information to better understand the mechanisms underlying rainfall variability.

Overall, the results demonstrate that rainfall variability in Jakarta is governed by complex interactions between long-term climate trends, abrupt changes, and seasonal dynamics. The application of a Bayesian changepoint framework provides a robust approach for uncovering these patterns and offers valuable insights for climate risk assessment in rapidly urbanizing tropical regions.

6. CONCLUSIONS

This study characterized the long-term variability and structural changes in monthly rainfall over Jakarta using a 161-year record spanning 1864–2024 and the Bayesian Estimator of Abrupt Change, Seasonality, and Trend (BEAST). The results demonstrate that the rainfall series exhibits persistent seasonal variability accompanied by temporal changes in both the long-term trend and seasonal structure, indicating that the rainfall regime has not remained stationary throughout the observation period.

The BEAST analysis identified probabilistic structural changepoints in both the trend and seasonal components. The principal trend transition occurred around 2020, while the seasonal component exhibited notable changes around 2014 and 2016. These findings indicate that changes in Jakarta rainfall have occurred not only in its long-term behavior but also in the magnitude of its seasonal cycle. The detected changepoints provide evidence of non-stationary rainfall behavior and highlight periods in which the underlying rainfall structure changed substantially.

The analysis also identified isolated extreme observations through the explicit outlier component. The sensitivity analysis showed that accounting for these extreme observations reduced the posterior support and magnitude of several detected changepoints, particularly the transition around 2020. Nevertheless, the principal structural changes remained identifiable after the outlier component was incorporated. This indicates that extreme observations influence the strength of the detected structural changes but do not fully account for the observed non-stationary behavior.

Overall, the findings demonstrate that the long-term Jakarta rainfall record is characterized by changing trend and seasonal structures together with isolated extreme observations. The combination of probabilistic changepoint detection and explicit outlier treatment therefore provides a useful framework for distinguishing persistent changes in rainfall behavior from individual extreme events and can support subsequent non-stationary rainfall and extreme-value analyses.

Future research should extend this framework by integrating climate drivers, such as sea surface temperature variability and large-scale climate indices. It should also incorporate land-use changes to better explain the mechanisms underlying rainfall variability. Furthermore, expanding the analysis to multi-station datasets would enhance the robustness and generalizability of the findings.

ACKNOWLEDGEMENTS.

This research has been funded by BIMA Kemendikbudristek program through the scheme “Penelitian Fundamental Reguler (PFR)” with contract number 006/C3/DT.05.00/PL/2025. In addition, we also thank the Division of Computational Mathematics, School of Data Science, Mathematics, and Informatics, IPB University, Bogor, Indonesia, for the support provided in this research.

REFERENCES

ADINET (2013) Indonesia: Flood affecting Jakarta. ASEAN Coordinating Centre for Humanitarian Assistance on Disaster Management (AHA Centre). Available from: https://adinet.ahacentre.org/report/indonesia-flood-affecting-Jakarta-20130507 [Accessed 19th September 2025].

Aguilar, E., Auer, I., Brunet, M., Peterson, T.C. and Wieringa, J. (2003). *Guidelines on Climate Metadata and Homogenization*. WMO-TD No. 1186, WCDMP No. 53. Geneva: World Meteorological Organization.

Aldrian, E., & Susanto, R.D. (2003) Identification of three dominant rainfall regions within Indonesia and their relationship to sea surface temperature. *International Journal of Climatology*, 23(12), 1435–1452. doi:10.1002/joc.950

Allen, M.R., & Stott, P.A. (2003) Estimating signal amplitudes in optimal fingerprinting, part I: theory. *Climate Dynamics,* 21, 477–491. doi: 10.1007/s00382-003-0313-9

An, D., Eggeling, J., Zhang, L., He, H., Sapkota, A., Wang, Y.-C. and Gao, C. (2023). ‘Extreme precipitation patterns in the Asia-Pacific region and its correlation with El Niño-Southern Oscillation (ENSO)’, *Scientific Reports*, 13, 11068. doi:10.1038/s41598-023-38317-0

Anshory, W.W. (2025) Hujan deras di musim kemarau: Penjelasan BMKG terkait cuaca ekstrem. *Kompas.com*. Available from: https://www.kompas.com/jawa-barat/read/2025/07/07/211000688/hujan-deras-di-musim-kemarau-ini-penjelasan-bmkg-soal-cuac-ekstrem [Accessed 15th September 2025].

Berg, P., Haerter, J.O., Thejll, P., Piani, C., Hagemann, S., & Christensen, J.H. (2009) Seasonal characteristics of the relationship between daily precipitation intensity and surface temperature. *Journal of Geophysical Research: Atmospheres*, 114, D18. doi:10.1029/2009JD012008

Blain, G.C. (2011) Modeling extreme minimum air temperature series under climate change conditions. *Ciência Rural*, 41(11), 1877–1883. doi:10.1590/S0103-84782011001100005

Badan Meteorologi, Klimatologi, Dan Geofisika (BMKG). Pedoman Pengamatan Meteorologi; BMKG: Jakarta, Indonesia, 2020.

Bône, C., Gastineau, G., Thiria, S., & Gallinari, P. (2022) Detection and attribution of climate change: A deep learning and variational approach. *Environmental Data Science*, 1, e27. doi:10.1017/eds.2022.17

BPS (2018) *Provinsi DKI Jakarta dalam angka 2018*. Badan Pusat Statistik, Jakarta. Available from: https://jakarta.bps.go.id/id/publication/2018/08/16/67d90391b7996f51d1c625c4/provinsi-dki-jakarta-dalam-angka-2018.html [Accessed 21th October 2025].

Dan’azumi, S., Mamudu, L., & Aldrees, A. (2025) Climate change detection and attribution using BEAST and Mann–Kendall approaches. *Journal of Water and Climate Change*, 16(5), 1895–1912. doi:10.2166/wcc.2025.107972

Gilleland, E., & Katz, R.W. (2006) *extRemes: An R package for analyzing extreme weather and climate events*. Technical report. Available from: https://api.semanticscholar.org/CorpusID:2219833 [Accessed 15th September 2025].

Gocic, M., & Trajkovic, S. (2013) Analysis of changes in meteorological variables using Mann–Kendall and Sen’s slope estimator. *Global and Planetary Change*, 100, 172–182. doi:10.1016/j.gloplacha.2012.10.014

Gure, A. (2021) The role of climate information and early warning systems in disaster risk reduction. Technical report, WASH Cluster Somalia, 1-50.

Hammerling, D., Katzfuss, M., & Smith, R. (2019) Climate change detection and attribution. In: Collett, T., & Davison, A.C. (Eds.), *Handbook of Environmental and Ecological Statistics*, pp. 29–52. doi:10.1201/9781315152509-38

IPCC (2014) Observations: Atmosphere and surface. In: *Climate Change 2013: The Physical Science Basis*. Cambridge University Press, pp. 159–254. doi:10.1017/CBO9781107415324.008

IPCC (2023) *Climate Change 2023: Synthesis Report*. Available from: https://www.ipcc.ch/report/ar6/syr/ [Accessed 9th September 2025].

Iskandar, I., Lestari, D.O. and Nur, M. (2019). 'Impact of El Niño and El Niño Modoki Events on Indonesian Rainfall', *Makara Journal of Science*, 23(4), Article 7, pp. 217–222. doi:10.7454/mss.v23i4.11517

Islam, M.A., Chan, A., Ashfold, M.J., Ooi, C.G. and Azari, M. (2018). 'Effects of El-Niño, Indian Ocean Dipole, and Madden-Julian Oscillation on surface air temperature and rainfall anomalies over Southeast Asia in 2015', *Atmosphere*, 9(9), 352. doi:10.3390/atmos9090352

Jannah, M., Sujono, J., & Rahardjo, A.P. (2023) Kajian perubahan iklim di DKI Jakarta berdasarkan data curah hujan. *Teknisia*, 28(1), 43–54.

Januari, A.D., Rusdayanti, N., Kardian, S., & Shara, S. (2024) Urbanisasi Jakarta dan dampaknya terhadap sosial ekonomi dan lingkungan. *Sustainable Transportation and Urban Mobility*, 1(1), 21–37. Available from: https://journal-iasssf.com/index.php/STUM/article/view/448/471 [Accessed 21th October 2025].

Knutson, T.R., Zeng, F., & Wittenberg, A.T. (2013a) Extreme temperature anomaly over the eastern United States. *Bulletin of the American Meteorological Society*, 94(9), S13–S16.

Knutson, T.R., Zeng, F., & Wittenberg, A.T. (2013b) Multimodel assessment of temperature trends. *Journal of Climate*, 26(22), 8709–8743. doi:10.1175/JCLI-D-12-00567.1

Knutson, T., Kossin, J., Mears, C., Perlwitz, J., & Wehner, M. (2017) Detection and attribution of climate change. In: Wuebbles, D.J. et al. (Eds.), *Climate Science Special Report*, pp. 160–185. Available from: https://digitalcommons.unl.edu/usdeptcommercepub/590/ [Accessed 15th September 2025].

Koutsoyiannis, D., & Baloutsos, G. (2000) Analysis of a long record of annual maximum rainfall in Athens, Greece, and design rainfall inferences. *Natural Hazards*, 22, 29–48. doi:10.1023/A:1008001312219

Kunkel, K.E., & Coauthors (2013) Monitoring and understanding trends in extreme storms: state of knowledge. *Bulletin of the American Meteorological Society*. 94 (4), 499–514. doi:10.1175/BAMS-D-11-00262.1

Lubis, S.W., Hagos, S., Hermawan, E., Respati, M.R., Ridho, A., Risyanto, Paski, J.A.I., Muhammad, F.R., Siswanto, Ratri, D.N., Setiawan, S. and Permana, D.S. (2022). 'Record-breaking precipitation in Indonesia's capital of Jakarta in early January 2020 linked to the northerly surge, equatorial waves, and MJO', *Geophysical Research Letters*, 49(22), e2022GL101513. doi:10.1029/2022GL101513

Maheng, D., Bhattacharya, B., Zevenbergen, C., & Pathirana, A. (2024) Changing urban temperature and rainfall patterns in Jakarta: a comprehensive historical analysis. *Sustainability*, 16(1), 350. doi:10.3390/su16010350

Mardiana, A. (2025) Banjir Jakarta 2025. *Katadata*. Available from: https://katadata.co.id [Accessed 5th September 2025].

Min, S.-K., Kim, Y.-H., Kim, M.-K., & Park, C. (2014) Heat wave attribution. *Bulletin of the American Meteorological Society*, 95, S48–S51.

Muhammad, F.R., Lubis, S.W. and Setiawan, S. (2021). 'Impacts of the Madden–Julian oscillation on precipitation extremes in Indonesia', *International Journal of Climatology*, 41(3), pp. 1970–1984. doi:10.1002/joc.6941

Nguyen, M.T., Sebesvari, Z., Souvignet, M., Bachofer, F., Nguyen, H.Q. & Hagenlocher, M. (2021) Understanding and assessing flood risk in Vietnam: current status, persisting gaps, and future directions. *Journal of Flood Risk Management*. 14, e12689. doi:10.1111/jfr3.12689

Nurdiati, S., Najib, M.K., Thalib, A., & Syarief (2022) Dry days and precipitation probability. *Geographia Technica*, 17(2), 107–118. doi:10.21163/GT_2022.172.10

OCHA (2013) Humanitarian bulletin: Indonesia disaster incidence and impact fell as severe wet season draws to close. Technical report, 02.

Patel, K. (2020) Torrential rains flood Indonesia. NASA Earth Observatory. Available from: https://earthobservatory.nasa.gov [Accessed 5th September 2025].

Pettitt, A.N. (1979) A non-parametric approach to the change-point problem. *Applied Statistics*, 28, 126–135. doi:10.2307/2346729

Raidi (2025) Severe floods hit Jakarta metropolitan area. *Indonesia Sentinel*. Available from: https://indonesiasentinel.com [Accessed 5th September 2025].

Ribes, A., Zwiers, F.W., Azaïs, J.-M., & Naveau, P. (2017) A new statistical approaches to climate detection detection and attribution. *Climate Dynamics*, 48, 367–386. doi:10.1007/s00382-016-3079-6

Septiawan, P., Nurdiati, S., & Sopaheluwakan, A. (2017) Analisis empirical orthogonal function (EOF) dan transformasi Fourier pada sinyal curah hujan Indonesia. INA-Rxiv. doi:10.31227/osf.io/8e2f3

Setyawati, S.N., Nurdiati, S., Mangku, I.W., Haidu, I. & Najib, M.K. (2025) Time-varying bivariate modeling for predicting hydrometeorological trends in Jakarta using rainfall and air temperature data. *Hydrology*. 12, 252. doi:10.3390/hydrology12100252

Siliverstovs, B., Ötsch, R., Kemfert, C., Kolb, M. & Welsch, H. (2010) Climate change and modelling of extreme temperatures in Switzerland. *Stochastic Environmental Research and Risk Assessment*. 24, 311–326. doi:10.1007/s00477-009-0321-3

Sillmann, J., Kharin, V.V., Zwiers, F.W., Zhang, X. & Bronaugh, D. (2013) Climate extremes indices in the CMIP5 multimodel ensemble: Part 2. Future climate projections. *Journal of Geophysical Research: Atmospheres*. 118, 2473–2493. doi:10.1002/jgrd.50188

Siswanto, van Oldenborgh, G.J., van der Schrier, G., Lenderink, G. & van den Hurk, B. (2015) Trends in high-daily precipitation events in Jakarta and the flooding of January 2014. *Bulletin of the American Meteorological Society*. 96, S131–S135. doi:10.1175/BAMS-D-15-00128.1

Siswanto, S., van Oldenborgh, G.J., van der Schrier, G., Jilderda, R. & van den Hurk, B. (2016) Temperature, extreme precipitation, and diurnal rainfall changes in the urbanized Jakarta city during the past 130 years. *International Journal of Climatology*. 36, 3207–3225. doi:10.1002/joc.4548

Siswanto, van der Schrier, G., van Oldenborgh, G.J., van den Hurk, B., Aldrian, E., Swarinoto, Y., Sulistya, W. & Sakya, A.E. (2017) A very unusual precipitation event associated with the 2015 floods in Jakarta: an analysis of the meteorological factors. *Weather and Climate Extremes*. 16, 23–28. doi:10.1016/j.wace.2017.03.003

Siswanto, van der Schrier, G., & van den Hurk, B. (2022) Observed increase of urban extreme rainfall as surface temperature rise: The Jakarta case. *Journal of the Meteorological Society of Japan*, 100(3), 475–492. doi:10.2151/jmsj.2022-023

Skliris, N., Marsh, R., Haigh, I. D., Wood, M., Hirschi, J., Darby, S., Nguyen, P. Q., & Nguyen, N. H. (2022) Drivers of rainfall trends in and around Mainland Southeast Asia. *Frontiers in Climate*, 4, 926568. doi:10.3389/fclim.2022.926568

Spekkers, M., Rözer, V., Thieken, A., ten Veldhuis, M.-C. & Kreibich, H. (2017) A comparative survey of the impacts of extreme rainfall in two international case studies. *Natural Hazards and Earth System Sciences*. 17 (8), 1337–1355. doi:10.5194/nhess-17-1337-2017

Stott, P.A., & Mitchell, J.F.B. (2021) Detection and attribution of climate change. *Weather*, 76, 324. doi:10.1002/wea.4027

Suroso, I.A.G. & Santoso, P.B. (2021) Detection of trend behaviour of extreme rainfall over Java using Mann-Kendall. *IOP Conference Series: Earth and Environmental Science*. 698, 012010. doi:10.1088/1755-1315/698/1/012010

Templ, M., Kowarik, A. and Filzmoser, P. (2011). 'Iterative stepwise regression imputation using standard and robust methods', *Computational Statistics & Data Analysis*, 55(10), pp. 2793–2806. doi:10.1016/j.csda.2011.04.012

Tu, J., Wen, J., Yang, L.E., Reimuth, A., Young, S.S., Zhang, M., Wang, L., Garschagen, M. (2023) Assessment of building damage and risk under extreme flood scenarios in Shanghai. *Natural Hazards and Earth System Sciences*, 23, 3247–3260. doi:10.5194/nhess-23-3247-2023

van de Vyver, H. (2012) Evolution of extreme temperatures in Belgium since the 1950s. *Theoretical and Applied Climatology*, 107, 113–129. doi:10.1007/s00704-011-0456-2

Wicaksono, A., & Herdiansyah, H. (2019) The impact analysis of flood disaster in dki jakarta: Prevention and control perspective. *Journal of Physics: Conference Series*, 1339, 012092. doi:10.1088/1742 6596/1339/1/012092

World Meteorological Organization (WMO) (2021) New climate report is a clarion call for urgent action. Available from: https://wmo.int/news/media-centre/wmo-new-climate-report-clarion-call-urgent-action [Accessed 5th September 2025].

Yunika, A., Babel, M.S., & Takizawa, S. (2012) Watershed hydrological analysis of jakarta extreme floods. *Jurnal Teknik Sipil*, 12(1), 66–74. doi:10.24002/jts.v12i1.622

Zhang, C., Li, W., & Chen, J. (2013) Hyperspectral remote sensing of plant biochemistry using Bayesian model averaging with variable and band selection. *Remote Sensing of Environment*, 132, 102–119. doi:10.1016/j.rse.2012.12.026

Zhao, K. (2025) *Rbeast: Bayesian change-point detection and time series decomposition* [Computer software]. GitHub. Available from: https://github.com/zhaokg/Rbeast [Accessed 4th July 2025].

Zhao, X., Cheng, T., Duan, Z., Ma, Y., Li, X. & Huang, C. (2019) Detecting change-point, trend, and seasonality in satellite time series data to track abrupt changes and nonlinear dynamics: a Bayesian ensemble algorithm. *Remote Sensing of Environment*. 232, 111181. doi:10.1016/j.rse.2019.04.034

Zhou, X.H., Zhou, A., & Shen, S.L. (2023) How to mitigate the impact of climate change on modern cities: lessons from extreme rainfall. *Smart Construction and Sustainable Cities*, 1, 7. doi:10.1007/s44268-023-00009-z